Genome-Wide Identification of the DGK Gene Family in Kiwifruit (Actinidia valvata Dunn) and Expression Analysis of Their Responses to Waterlogging Stress

Meijuan Zhang , Cuixia Liu * , Faming Wang , ShiBiao Liu , Jianyou Gao , Jiewei Li , Quanhui Mo , Kaiyu Ye , Beibei Qi , Hongjuan Gong

Posted Date: 23 February 2024

doi: 10.20944/preprints202402.1396.v1

Keywords: diacylglycerol kinase; Actinidia valvata; phylogenetic analysis; waterlogging stress; expression pattern

Article

Genome-Wide Identification of the *DGK* Gene Family in Kiwifruit (*Actinidia valvata* Dunn) and Expression Analysis of Their Responses to Waterlogging Stress

Meijuan Zhang [1,2], Cuixia Liu [1,*], Faming Wang [1], ShiBiao Liu [3], Jianyou Gao [1], Jiewei Li [1], Quanhui Mo [1], Kaiyu Ye [1], Beibei Qi [1] and Hongjuan Gong [1]

[1] Guangxi Key Laboratory of Plant Functional Phytochemicals and Sustainable Utilization, Guangxi Institute of Botany, Guangxi Zhuang Autonomous Region and Chinese Academy of Sciences, Guilin 541006, China; liucuixia@gxib.cn (C.L.); 36326266@qq.com (F.W.); gjy@gxib.cn (J.G.); lijw@gxib.cn (J.L.); 532612040@qq.com (Q.M.); 584003811@qq.com (K.Y.); gongjian-3000@sohu.com (H.G.)

[2] College of Biology Pharmacy and Food Engineering, Shangluo University, Shangluo 726000, China; zmj521good@163.com (M.Z.)

[3] College of Biology and Environmental Sciences, Jishou University, Xiangxi, 416000, China; liushibiao_1@163.com (S.L.)

* Correspondence: liucuixia@gxib.cn

Abstract: Diacylglycerol kinase (DGK) is a lipid kinase that phosphorylates diacylglycerol (DAG) to generate phosphatidic acid (PA). Based on converting one important signaling molecule (DAG) to another (PA), DGK plays an important role in plant responses to abiotic stress including waterlogging stress. However, no studies have been reported on the characterization of the *DGK* gene family in the waterlogging-tolerant kiwifruit germplasm, *Actinidia valvata* Dunn. Here, we identified 18 *AvDGK* genes in the *A. valvata* genome. The phylogenetic analysis showed that AvDGKs can be classified into three clusters, and members within the same cluster have similar domain distribution, exon-intron structures and conserved motif compositions. Chromosome localization analysis revealed that all the *AvDGK* genes are located across 18 different chromosomes. There were 29 duplicated gene pairs in kiwifruit and all had undergone purifying selection during evolution. Promoter cis-element analysis revealed that the cis-elements within *AvDGK* genes are associated with multiple functions, including phytohormone signal transduction, stress response, and plant growth and development. The expression pattern analyses indicated that AvDGK play an important role in the fruit development and plant response to waterlogging stress. *AvDGKs* gene family in the tetraploid *A. valvata* genome might promote PA synthesis and subsequent signal transduction both under short-term and long-term waterlogging stress. These results provide information regarding the structural characteristics and potential function of *DGK* genes within kiwifruit and lay a fundamental basis for further research into breeding for enhancing the kiwifruit's tolerance to waterlogging stress.

Keywords: diacylglycerol kinase; *Actinidia valvata*; phylogenetic analysis; waterlogging stress; expression pattern

1. Introduction

As the main components of cellular membranes, lipids also play a crucial role in cellular signal transduction. Among them, phosphatidic acid (PA) is an important signaling lipid molecule and its cellular level fluctuates rapidly and transiently in response to various biotic and abiotic stresses [1–6]. The production of PA can be rapidly triggered in response to stimuli such as calcium [7,8], abscisic acid (ABA) [9], reactive oxygen species (ROS) [10], and other factors. As the simplest phospholipid, PA can be produced by hydrolyzing membrane phospholipids such as phosphatidylcholine (PC) by phospholipase D (PLD). Moreover, PA can also be synthesized by diacylglycerol kinase (DGK) by phosphorylating diacylglycerol (DAG) which is another main signaling molecule within eukaryotic

 doi:10.20944/preprints202402.1396.v1

cells. Therefore, based on converting one important signaling molecule (DAG) to another (PA), DGKs play important roles in the regulation of plant growth, development and adaption to the environmental stresses [11–14].

DGKs are a widespread family of enzymes in most multicellular organisms. Members of *DGK* gene family have been identified in various plant species, including *Arabidopsis thaliana* [14], *Oryza sativa* [15], *Phaseolus vulgaris* [16], *Brassica napus* [17], *Triticum aestivum* [18], *Malus domestica* [19], *Glycine max* [20], *Zea mays* [21], and *Populus trichocarpa* [22]. In plants, DGKs are grouped into three phylogenetic clusters based on their domain structures and sequence similarities [13,14]. DGKs in all clusters possess a conserved catalytic domain with an ATP-binding site (consensus GXGXXG/A) required for kinase activity [23]. Besides, Cluster I contained two C1-type domains, which are cysteine-rich domains, thought to be responsible for binding the substrate DAG [24].

The roles of DGKs in different clusters also exhibit functional variations. In *Arabidopsis*, AtDGK1 groups together with AtDGK2 in Cluster I on the phylogenetic tree which is expressed in the roots, leaves, and shoots, but not in the flowers and siliques [12,25]. Conversely, the expression of AtDGK4 and AtDGK7 in Cluster II is strongest in flowers [26]. Similarly, OsDGK1 modulates the root architecture of rice by altering the density of lateral and seminal roots [27]. In response to stress, the expression of *AtDGK2* is transiently induced by wounding and cold stress [23], while the expression of *AtDGK5* (Cluster III) increased under water and salt stress [28]. Moreover, AtDGK5 is involved in regulating ROS production in plant immunity [2]. Furthermore, *AtDGK1* and *AtDGK5* were rapidly upregulated within 10 minutes after submergence, indicating that DGK may play vital role in short-term accumulation of PA under waterlogging stress [29].

Kiwifruit is widely favored for its high content of vitamin C, rich mineral elements, and delicious taste. Belonging to *Actinidia*, a large genus that contains more than 50 species provides a great diversity of genetic resources for development of new kiwifruit cultivars [30–32]. Among them, *Actinidia valvata* Dunn. is a shrub mainly growing in eastern China. Increasing evidence suggests that the greater tolerance to waterlogging stress has been observed in *A. valvata* which is commonly used as a rootstock [33–35]. However, the tolerance mechanism of *A. valvata* rootstocks' adaptation to waterlogging stress has not been clarified. Therefore, it is necessary to identify the *DGK* gene family in *A. valvata* and explore the role of *AvDGK* under waterlogging stress. In this study, we systematically identified and characterized the *DGK* family members in *Actinidia valvata*. Additionally, we investigated the expression patterns of *AvDGKs* at different fruit development stages and under salt stress, and their potential roles under waterlogging stress. Our findings provide information regarding the structural characteristics and potential function of *DGK* genes within kiwifruit and fundamental basis for further breeding research aimed at enhancing the tolerance in kiwifruit under waterlogging stress.

2. Materials and Methods

2.1. Identification of DGK genes in kiwifruit (Actinidia valvata)

We used the kiwifruit (*Actinidia valvata*) genome (unpublished) to identify and characterize the *DGK* genes. Two methods, blastp and hmmsearch, were employed to identify the *DGK* genes in kiwifruit. Seven DGK protein sequences of *Arabidopsis thaliana* (AtDGK) was downloaded from the TAIR database (https://www.arabidopsis.org/) [36] and used for BlASTp against the kiwifruit protein sequences. The DGK domains, including the diacylglycerol kinase catalytic (DAGK_cat/DAGKc/DGKc) domain (PF00781) and diacylglycerol kinase accessory (DAGK_acc/DAGKa/DGKa) domain (PF00609), were obtained from the Pfam database (https://pfam.xfam.org/) [37]. These two domains were used to search the kiwifruit protein database using HMMER 3.0 (https://www.ebi.ac.uk/Tools/hmmer/) [38]. The results of these two methods were merged and submitted to NCBI-CDD website (https://www.ncbi.nlm.nih.gov/cdd), Pfam and SMART databases (http://smart.embl-heidelberg.de/) to further confirm the DGK-conserved domains in each putative protein.

 doi:10.20944/preprints202402.1396.v1

2.2. Physiochemical properties, protein secondary structure and 3D modeling of AvDGK proteins

The physical and chemical properties of the AvDGK proteins, including amino acid (A.A) length, molecular weight (M.W), isoelectric point (pI), were evaluated using the ExPASy website (https://www.expasy.org/). Cell-ploc 2.0 (http://www.csbio.sjtu.edu.cn/bioinf/Cell-PLoc-2/) [39] was used to predict the subcellular localization of AvDGK proteins. The secondary structures of AvDGK proteins were predicted using SOPMA (http://npsa-pbil.ibcp.fr/cgi-bin/npsa_automat.pl?page=npsa_sopma.html) [40]. Furthermore, we utilized the online tool Phyre2 (http://www.sbg.bio.ic.ac.uk/phyre2/html/page.cgi?id=index) [41] for protein homology modeling and generation of 3D models of AvDGK proteins using default parameters. The protein domains were analyzed using the SMART database, and the domain structures in all AvDGK proteins were plotted using IBS 1.0.3 software [42].

2.3. Phylogenetic analyses and multiple sequence alignment of AvDGK proteins

The 7 AtDGK protein sequences were downloaded from the TAIR database (https://www.arabidopsis.org/), 7 ZmDGKs were obtained from the maize protein database (*Zea mays*, http://www.maizegdb.org/), 7 PtDGKs were obtain from Phytozome v13 (*Populus trichocarpa*, https://phytozome-next.jgi.doe.gov/) [43], and 9 AchDGKs were obtained by BlASTp from the whole protein sequences of *Actinidia chinensis* 'Hongyang' with AtDGKs. Multiple sequence alignment of these DGK proteins was performed using the Clustal W method with default setting, and then phylogenetic tree was constructed using MEGA 7.0 software with the neighbor-joining (NJ) method based on the result of sequence alignment. Bootstrap analysis with 1000 replicates was performed, and the phylogenetic trees were visualized using the online web tool iTOL (https://itol.embl.de/) [44]. Multiple sequence alignment of DGK sequences were visualized using the online web tool ESPript 3.0 (https://espript.ibcp.fr/ESPript/cgi-bin/ESPript.cgi) [45].

2.4. Analysis of gene structures and conserved motifs

The coding sequences (CDS) and their corresponding genomic sequences of *AvDGK* genes were retrieved from *Actinidia valvata* genomic files. The conserved motifs of AvDGK protein sequences were predicted using the MEME (MEME 5.5.4) online tool (https://meme-suite.org/meme/tools/meme) [46] and the numbers of motifs were set to 10. The gene structures and conserved motifs of AvDGK were visualized by TBtools software [47].

2.5. Chromosome location, gene duplication, and collinearity analysis of AvDGK genes

The chromosomal localization of *AvDGK* genes was obtained from gff3 file of the genome and mapped on chromosomes using MG2C online software (http://mg2c.iask.in/mg2c_v2.1/) [48]. Gene duplication events were identified by generating syntenic blocks within and between kiwifruit genomes using the MCScanX program with default parameters [49], and collinearity of the *DGK* family members within *A. valvata* genomes and between *A. thaliana*, and kiwifruit (*A. valvata* and *A. chinensis*) was determined using TBtools software [47]. The Ka (synonymous) and Ks (nonsynonymous) substitution rates in duplicated *DGK* gene pairs were calculated using TBtools software [47].

2.6. Cis-regulatory element prediction and analysis of promoters

The 2,000 bp upstream sequences of *AvDGK* genes were extracted from the genomic DNA sequences and selected as promoter region. The promoter sequences were submitted to the PlantCARE (https://bioinformatics.psb.ugent.be/webtools/plantcare/html/) for predicting the cis-regulatory elements [50]. TBtools was used for visualizing the results of the analysis.

2.7. Gene expression analysis of AvDGKs

 doi:10.20944/preprints202402.1396.v1

Raw RNA-seq data of kiwifruit flesh from different fruit stages were downloaded from NCBI (https://www.ncbi.nlm.nih.gov/) with the following accession number (PRJNA984935). The transcriptome datasets (PRJNA726156) were obtained from NCBI to investigate the expression profiles of *AvDGKs* under salt stress. The expression levels were illustrated based on the log2 transformed FPKM values using Kallisto and visualized by TBtools [47,51].

2.8. Plant Materials and Treatments

Actinidia valvata seedlings were provided by Guangxi Key Laboratory of Plant Functional Phytochemicals and Sustainable Utilization and grown under normal conditions. For the waterlogging experiment, seedlings at the six-leaf stage were submerged to a final depth of 3~5 cm beneath the water surface for 5 days under a normal light-dark conditions. Fresh root samples were collected at 0, 6, 24, and 120 h after waterlogging treatment and immediately frozen in liquid nitrogen for further analysis.

2.9. RNA extraction and qRT-PCR analysis

Total RNA of the root samples was extracted using the RNAprep Pure Plant Kit (TIANGEN). The FastKing RT Kit With gDNase (TIANGEN) was employed to reverse RNA into cDNA. Following the protocol of SuperReal PreMix Plus (SYBR Green) (TIANGEN), each 20 μL reaction mixture contained 1 μL of template cDNA, 10 μL of the 2 × SuperReal PreMix Plus (SYBR Green), 0.6 μL of each primer, and 7.8 μL of ddH2O. The reaction conditions comprised a predenaturation at 95°C for 5 min, followed by 40 cycles of denaturation at 95°C for 10 sec, annealing at 60°C for 20 sec, and extension at 72°C for 20 sec. The *Actinidia valvata* Actin gene (AVa07g00333) was used as the reference gene. The relative expression levels were calculated using the $2^{-\Delta\Delta CT}$ method [52] and three duplicates were performed. All the primer pairs used for RT-PCR are listed in Table S1.

2.10. Statistical analysis

All statistical analyses were performed with Microsoft Excel software. The significance levels of data were checked by performing one-way ANOVA in SPSS (ANCOVA; SPSS26, SPSS Inc., Chicago, IL, United States), and * $P < 0.05$ and ** $P < 0.01$ indicated that the difference was significant and extremely significant. The data are presented as mean ± standard deviation (± SD). Each treatment was repeated three times.

3. Results

3.1. Genome-Wide Identification of DGK Genes in Kiwifruit

To identify the DGK family members in kiwifruit (*Actinidia valvata*), the DGK protein sequences from *Arabidopsis thaliana* were used as the query sequence to conduct the BLASTp search against kiwifruit genome database. Furthermore, HMMER software was utilized to search the DAGKa and DAGKc domains in the kiwifruit genome database. After these two methods, a total of 18 putative *AvDGK* genes were predicted, and their domains were confirmed using the NCBI CDD and SMART databases. Finally, all 18 candidate *AvDGK* genes were proved containing both functional domains and identified from the kiwifruit genome. Based on their chromosome position, they were named as *AvDGK5a/b*, *AvDGK7a/b*, *AvDGK12a/b*, *AvDGK13a/b*, *AvDGK16a/b*, *AvDGK17a/b*, *AvDGK18a/b*, *AvDGK19a/b*, and *AvDGK23a/b* (Figure 1, Table S2). The CDS lengths of *AvDGK* genes ranged from 1371bp to 2205bp and the length of the proteins were 456~734 amino acids (Table 1). Their molecular weights ranged from 50.84 to 81.06 kDa, and the pI values ranged from 6.31 to 9.16. The predicted subcellular localization of the proteins was in the nucleus, chloroplast and cytoplasm (Table 1).

 doi:10.20944/preprints202402.1396.v1

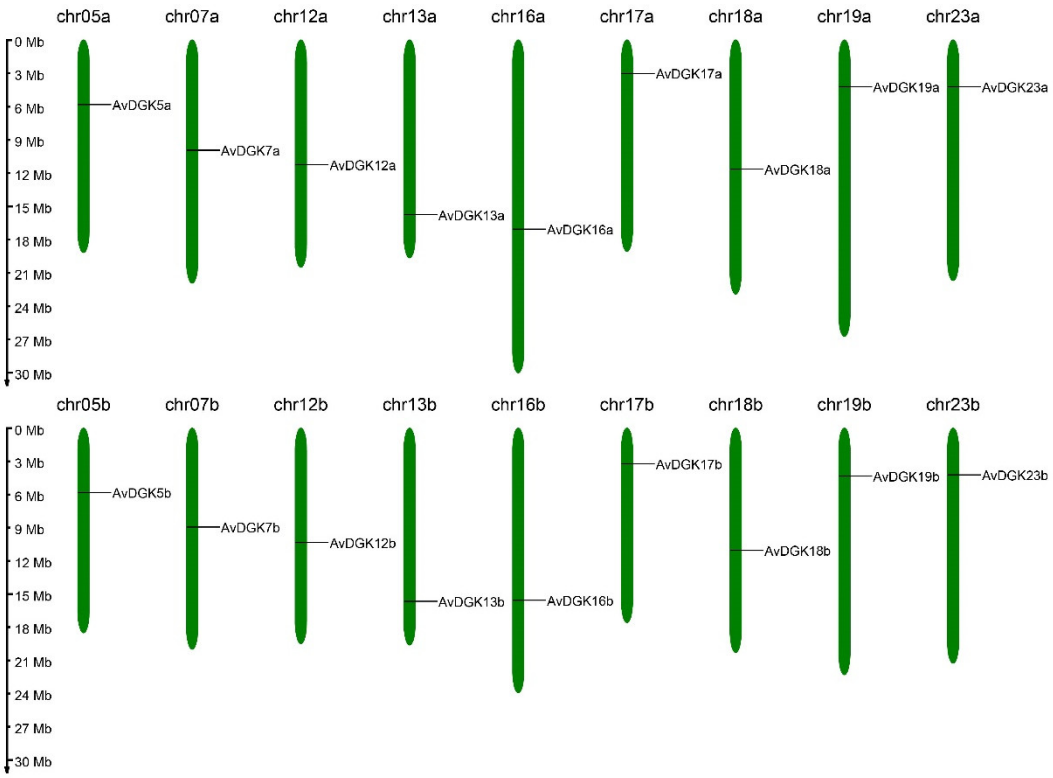

Figure 1. Chromosomal localization of *AvDGK* genes.

Table 1. The characteristics of the *DGK* family members in kiwifruit (*Actinidia valvata*).

Gene name	Gene ID	CDS length (bp)	Number of amino acids (aa)	Molecular weight (kDa)	pI	Subcellular Localiaztion
AvDGK5a	AVa05g00367	2139	712	79.50	8.62	Nucleus
AvDGK5b	AVb05g00366	2139	712	79.31	8.74	Nucleus
AvDGK7a	AVa07g00406	2139	712	79.24	8.14	Nucleus
AvDGK7b	AVb07g00371	2139	712	79.39	8.14	Nucleus
AvDGK12a	AVa12g00623	1449	482	54.05	8.57	Chloroplast. Cytoplasm. Nucleus
AvDGK12b	AVb12g00588	1392	463	51.84	7.06	Cytoplasm
AvDGK13a	AVa13g01333	1419	472	53.55	9.16	Chloroplast
AvDGK13b	AVb13g01246	1419	472	53.28	8.68	Chloroplast. Cytoplasm. Nucleus
AvDGK16a	AVa16g01104	1446	481	53.40	6.84	Chloroplast
AvDGK16b	AVb16g01069	1437	478	53.14	6.87	Chloroplast
AvDGK17a	AVa17g00287	1473	490	54.90	6.39	Chloroplast. Cytoplasm
AvDGK17b	AVb17g00295	1473	490	54.95	6.31	Cytoplasm. Nucleus
AvDGK18a	AVa18g00909	1446	481	53.53	6.72	Chloroplast
AvDGK18b	AVb18g00884	1371	456	50.84	6.41	Chloroplast
AvDGK19a	AVa19g00482	2199	732	80.77	6.32	Nucleus
AvDGK19b	AVb19g00480	2205	734	81.06	6.50	Nucleus
AvDGK23a	AVa23g00486	2205	734	80.91	6.44	Nucleus
AvDGK23b	AVb23g00493	2205	734	80.83	6.41	Nucleus

3.2. Phylogenetic Analysis and Multiple Sequence Alignment of DGK Genes

To elucidate the phylogenetic relationships and functional differences of the 18 AvDGKs, DGK protein sequences from other plants, including *Arabidopsis thaliana*, *Actinidia chinensis* 'Hongyang', *Zea mays* and *Populus trichocarpa* were used to conduct the multiple sequence alignment by Clustal W. Based on the alignment result, the phylogenetic tree of these DGK proteins was constructed with

 doi:10.20944/preprints202402.1396.v1

MEGA 7.0 using the neighbor-joining method. The results showed that the 18 AvDGK proteins were divided into three clusters (Figure 2). Cluster I included AvDGK5a/b, AvDGK7a/b, AvDGK19a/b and AvDGK23a/b; Cluster II contained AvDGK16a/b and AvDGK18a/b; Cluster III consisted of AvDGK12a/b, AvDGK13a/b, and AvDGK17a/b. The grouped results of phylogenetic tree were confirmed by the amino acid similarities between AtDGKs and AvDGKs (Figure S1). The phylogenetic tree also revealed that the AvDGKs had high homology with DGKs in *Actinidia chinensis* 'Hongyang', and *AvDGKs* are more closely related to *AchDGKs* located in the same chromosome of kiwifruit than to *DGKs* of other plants.

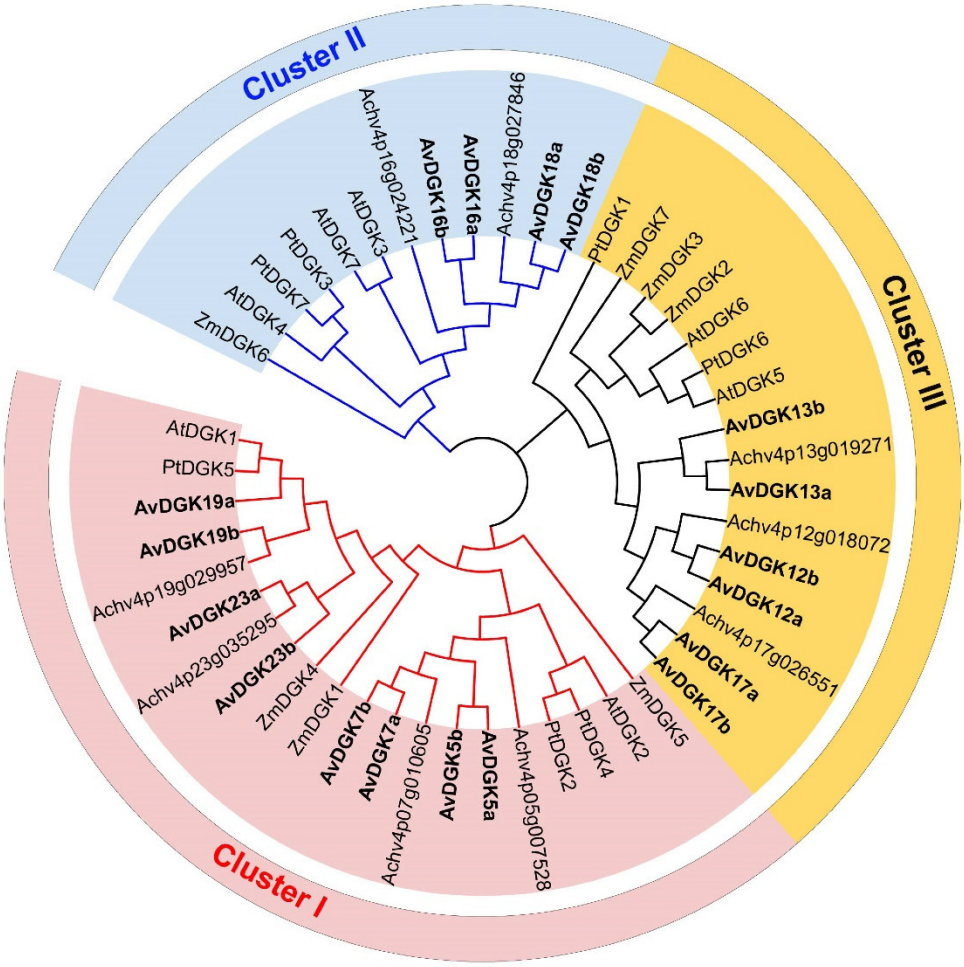

Figure 2. Phylogenetic tree analysis of the DGK proteins from kiwifruit (*Actinidia valvata*) (Av), kiwifruit (*Actinidia chinesis*) (Ach), *Arabidopsis thaliana* (At), *Populus trichocarpa* (Pt) and *Zea mays* (Zm). The protein sequences were aligned with the Clustal W program using MEGA 7.0 and the phylogenetic tree was constructed using the neighbor-joining method with 1000 bootstrap replicates.

To identify the conserved sequences in AvDGKs, multiple sequence alignment was performed using Clustal W, and the results were visualized using the online web tool ESPript 3.0. According to the alignment, a diacylglycerol kinase catalytic (DAGKc) domain (Figure 3A), a diacylglycerol kinase accessory (DAGKa) domain (Figure 3B) and two DAG/PE-binding domains (Figure 3C) were shown. The alignment revealed that almost all DGKs, except for the AtDGK2, AvDGK5a/b, AvDGK7a/b and AvDGK13a/b, contained the predicted ATP-binding site with a GXGXXG consensus sequence (G represents glycine and X represents any other amino acid) in the DAGKc domain. Furthermore, glycine (G) is replaced by alanine (A) in AtDGK2, AvDGK5a/b and AvDGK7a/b and by lysine (K) in AvDGK13a/b. The two C1 domains observed in Cluster I DGKs harbor the sequences

 doi:10.20944/preprints202402.1396.v1

HX14CX2CX19~22CX2CX4HX2CX7 and HX18CX2CX16CX2CX4HX2CX11C respectively (Figure 3D). Additionally, the upstream basic regions and the extended cysteine-rich (extCRD)-like domain were extremely conserved in Cluster I.

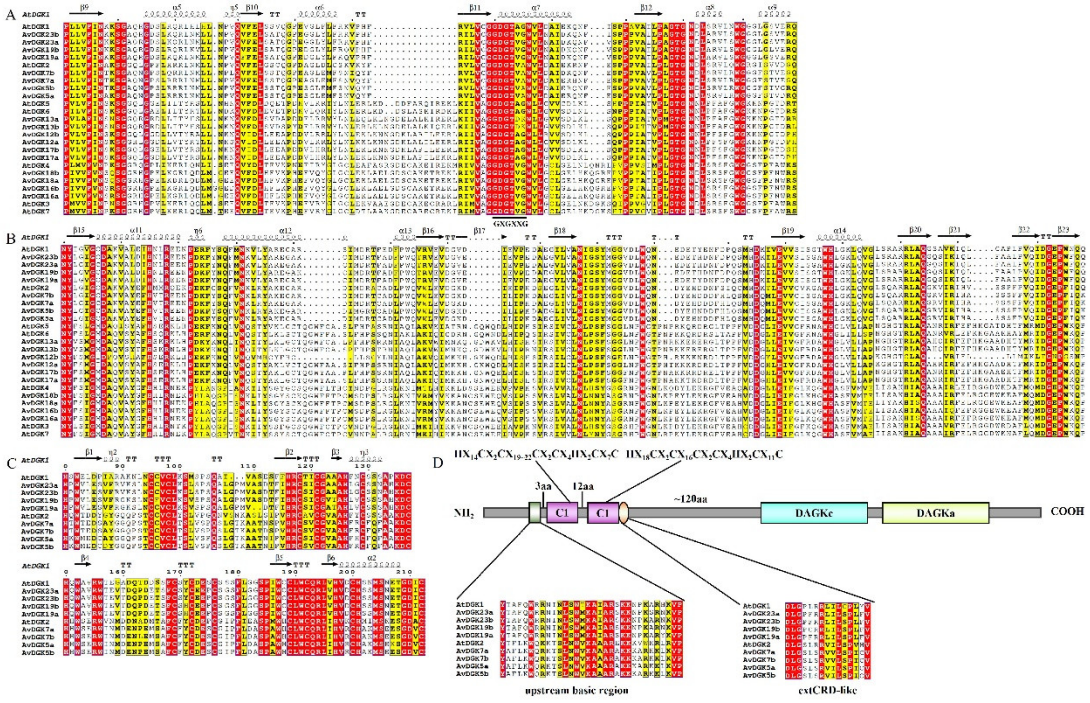

Figure 3. Multi-sequence alignment and domain analysis of AtDGK and AvDGK proteins. (A) DAGKc domain, the predicted ATP-binding site with a GXGXXG consensus sequence is showed below the DAGKc domain. (**B**) DAGKa domain, (**C**) DAG/PE-binding domains in DGKs. (D) A schematic diagram of *AvDGK* genes in cluster I. The conserved C6/H2 cores, the upstream basic regions and the extended cysteine-rich (extCRD)-like domain are shown in the schematic diagram.

3.3. Functional Domain, Secondary Structure, and 3D Modeling of AvDGKs

To further explore the protein domains in all AvDGKs, the functional domains of AvDGKs were predicted by SMART and their domain distributions were diagramed using the IBS software (Figure 4). The results showed that all DGK both had a DAGKc domain and a DAGKa domain. Additionally, DGK proteins in Cluster I (AvDGK5a/b, AvDGK7a/b, AvDGK19a/b and AvDGK23a/b) also contained two C1 domains. Based on the starting and ending positions of domains, AvDGK19a/b exhibit higher similarities with AvDGK23a/b than other DGKs in Cluster I. The domain position and distribution of AvDGK5a/b were completely consistent with AvDGK7a/b. Similar domain position and distribution were found in DGKs belonged in the same Cluster.

To develop a better understanding of DGK protein structure, the secondary structure of AvDGKs were predicted by the web tool SOPMA. The secondary structure of the AvDGK proteins was predominantly composed of alpha helices, extended strands, beta turns, and random coils (Figure S2, Table S3). The analysis showed that the random coils accounted for the largest percentage of secondary structures among all AvDGK proteins, followed by alpha helix and extended strands, while the beta turns accounted less than 6.0%. Besides, the 3D models of all AvDGKs proteins were predicted using the default mode of the Phyre server (Figure S3). Similar 3D structures were found in AvDGKs, and the composition and position of secondary structure could be clearly observed.

 doi:10.20944/preprints202402.1396.v1

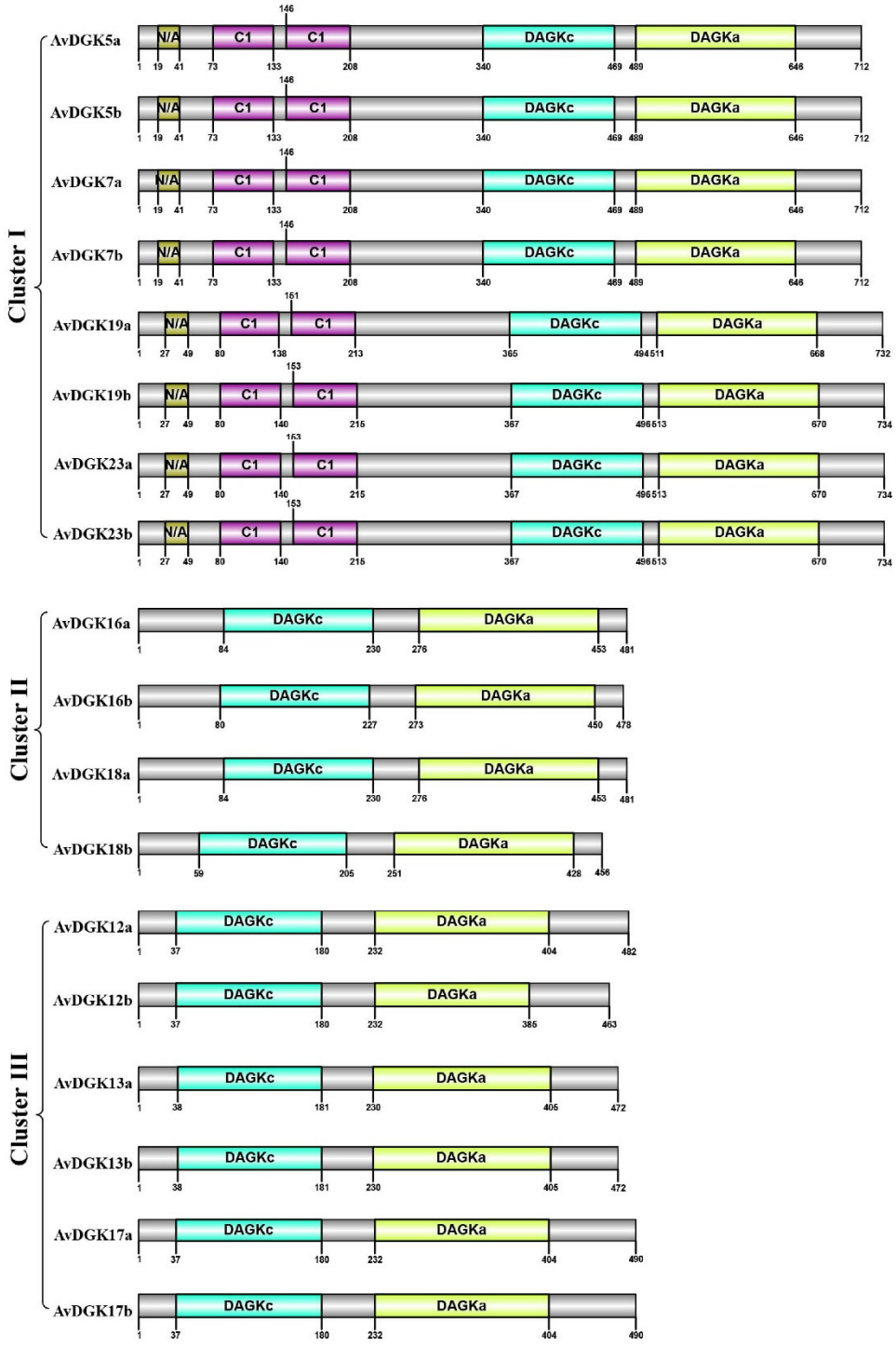

Figure 4. Distribution of the function domains in AvDGK proteins. The numbers up/down the protein indicate the position of each domain in the protein.

3.4. Gene Structure, Domain and Conserved Motifs Analysis of AvDGKs

To investigate the diversity and differentiation of AvDGKs, we further analyzed the gene structure and conserved motifs of AvDGK family. A total of 10 different conserved motifs, labeled as motif 1 to motif 10, were identified in AvDGKs (Figure 5B, Figure S4). Similar motif distribution was observed within a Cluster. According to the results, AvDGKs from Cluster I contained a maximum of 10 motifs, while AvDGKs from Cluster II contained a minimum 6 motifs (Figure 5B). The members

 doi:10.20944/preprints202402.1396.v1

of Cluster III contained one additional motif compared to the members of Cluster II, namely motif 10. The protein domains of AvDGKs were clearly shown in Figure 5C. All AvDGKs have a DAGKc domain and a DAGKa domain, and two C1 domains were conserved in Cluster I DGKs (Figure 5C). Gene structure of AvDGKs could provide insights into their classification and functional diversification. The *AvDGKs* genes belong to Cluster I possessed a smaller number of exons compared to other *AvDGKs* genes, which all contained 7 exons and 6 introns (Figure 5D, Figure S5). The Cluster II members (*AvDGK16a/b* and *AvDGK18a/b*) all contained 12 exons and 11 introns, whereas the exon numbers from Cluster III varied from 11 to 13 (Figure 5D, Figure S5).

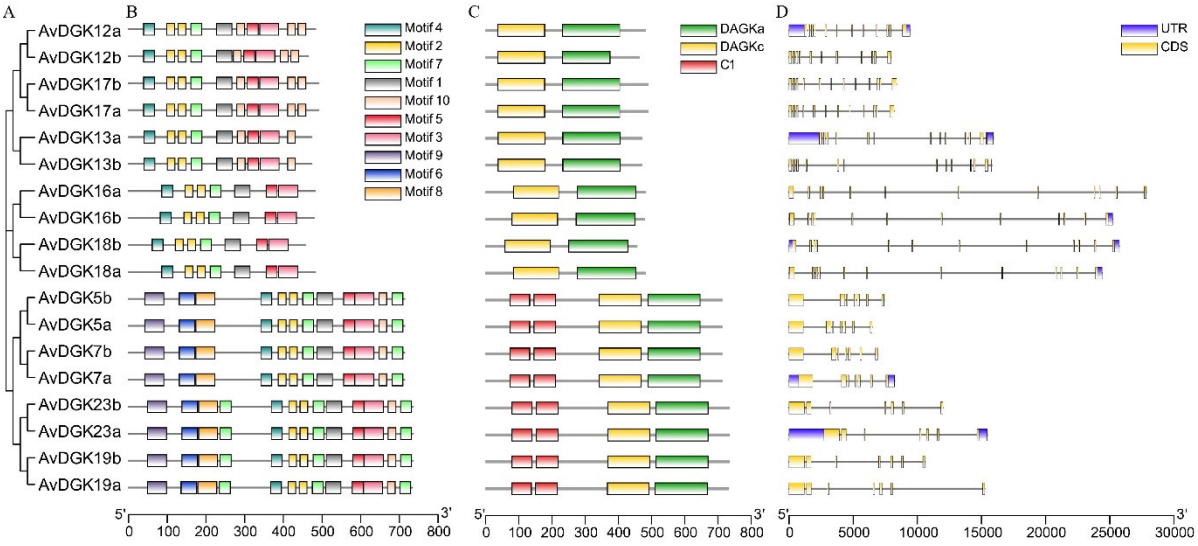

Figure 5. The phylogenetic tree, motif composition, domain location and gene structure of the AvDGKs. (**A**) The phylogenetic tree of the AvDGK proteins. (**B**) Conserved motifs distribution of the AvDGK proteins. (**C**) The domain location of the AvDGK proteins. (**D**) Gene structure of the *AvDGK* genes, yellow color indicates the exons, gray color lines indicate the introns, and the purple color shows the untranslated 5′ and 3′-regions.

3.5. Synteny and Gene Duplication Analysis of AvDGKs

To determine the expansion patterns of the *DGK* gene family, a collinearity analysis was performed to identify duplicated gene pairs for *DGK* genes in *A. valvata*. A total of 29 duplicated gene pairs were identified in the *A. valvata* genome (Figure 6 and Table S4). Among them, there were each 5 duplicated gene pairs respectively in subgenome a or subgenome b of *A. valvata*, and 19 duplicated gene pairs between subgenome a and subgenome b. We estimated the selection pressure of replication gene pairs by calculating nonsynonymous (Ka) and synonymous (Ks) substitution rates. Ka/Ks < 1 indicates purifying selection, Ka/Ks > 1 denotes positive selection, and Ka/Ks = 1 represents neutral selection [53,54]. The results showed that the Ka/Ks ratio for all duplicated gene pairs ranged from 0.11 to 0.85, indicating that the duplicated gene pairs in kiwifruit underwent purifying selection (Table S4). The results also suggested that the duplication events in *A. valvata* occurred between 4.67 to 76.36 million years ago (MYA) (Table S4).

 doi:10.20944/preprints202402.1396.v1

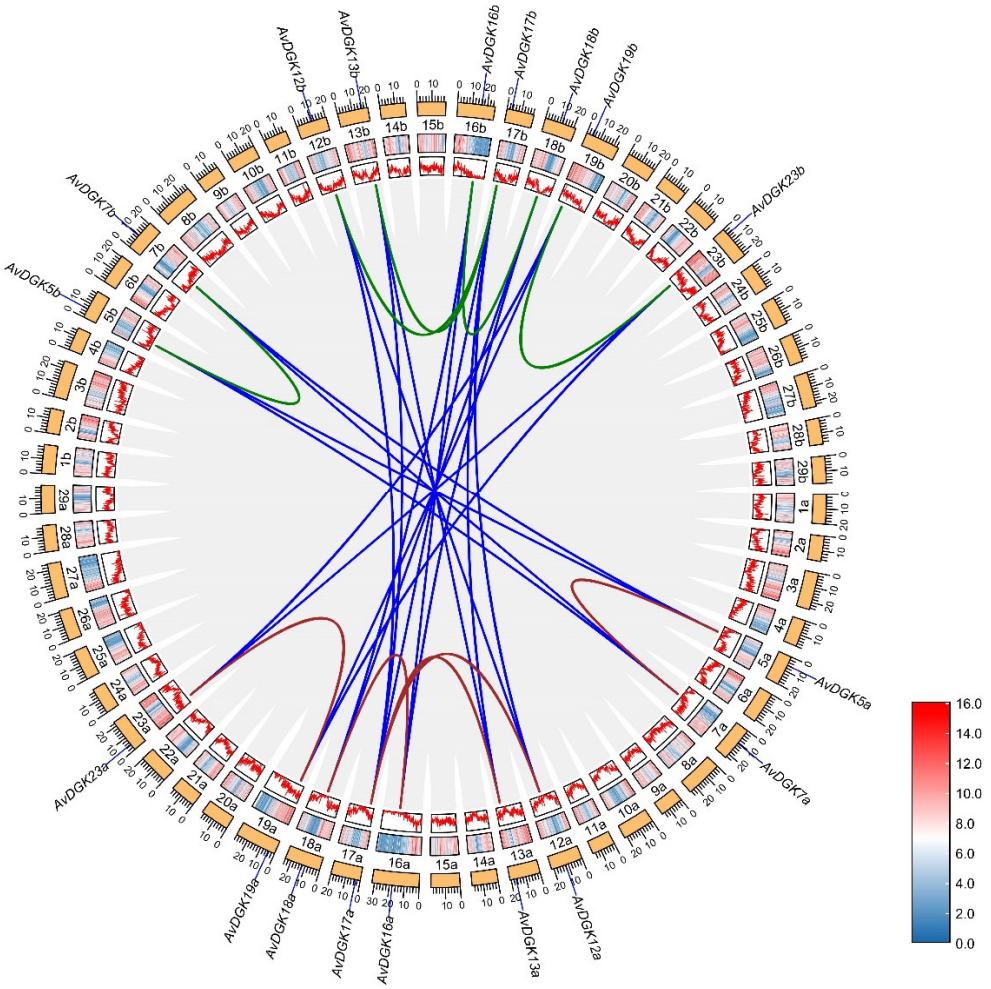

Figure 6. Collinearity analysis of *AvDGKs*. Grey lines indicate all duplicate genes, other different colored lines indicate the duplicated *DGK* gene pairs within and between *A. valvata* subgenomes. The heatmap and line graph means gene density.

To further understand the evolutionary origins and orthologous relationship of the *DGK* gene family, a collinearity analysis was performed among *A. valvata*, *Arabidopsis thaliana* and *Actinidia chinensis* 'Hongyang' (Figure 7). Nineteen gene pairs were found between between *A. valvata* subgenome a and subgenome b (Figure 7A). Each 18 gene pairs were found between between *A. valvata* subgenome and *Actinidia chinensis* 'Hongyang' (Figure 7B). The difference was that 11 and 10 gene pairs were found between *Arabidopsis thaliana* with *A. valvata* subgenome a and subgenome b (Figure 7C). The collinearity analysis provides insights into the evolutionary dynamics and functional divergence of the *DGK* gene family in *A. valvata* and related species.

 doi:10.20944/preprints202402.1396.v1

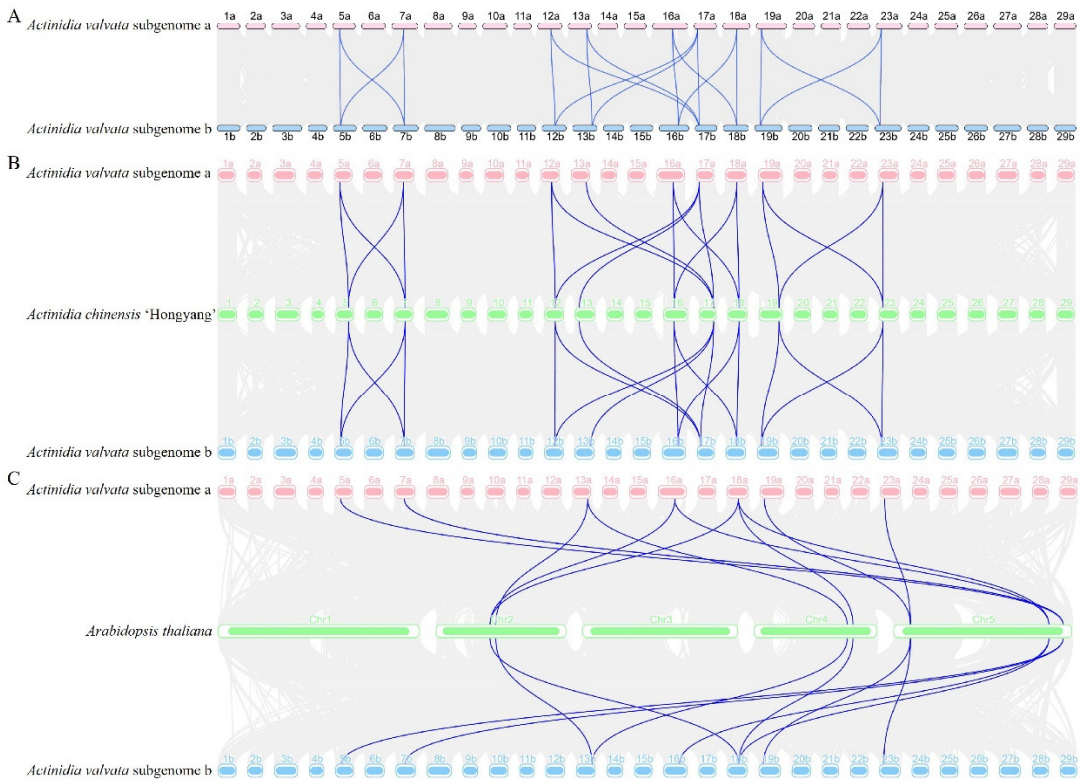

Figure 7. Multiple collinearity analysis between *A. valvata*, *A. thaliana* and *A. chinensis* 'Hongyang'. The grey lines in the background represent all the syntenic blocks between *A. valvata* subgenome and other plants, and the blue lines highlight the *DGK* genes orthologous in *A. valvata* subgenome and other plants.

3.6. Analysis of Cis-Elements in the Promoters of AvDGK genes

To explore the possible regulatory patterns of the *AvDGK* genes, the upstream 2,000 bp promoter sequences of all *AvDGK* genes were analyzed using PlantCARE. The putative cis-elements were involved in stress response, phytohormone regulation, and plant growth and development (Figure 8). The distribution and numbers of these cis-elements exhibited that the light responsiveness element was the most commonly occurring (Figure 8A). The phytohormone responsive cis-acting elements are also widely distributed, especially that MeJA responsiveness element which is present in almost all *AvDGK* genes. However, only six *AvDGK* promoters contained salicylic acid (SA) responsiveness elements. Moreover, cis-acting elements related to stress responses, such as wound stress responsiveness, drought responsiveness, low-temperature responsiveness, anaerobic induction, defense and stress responsiveness were also found in promoters of *AvDGK* genes (Figure 8A). Notably, hypoxia induces the expression of almost all *AvDGK* genes, except for *AvDGK18b* and *AvDGK19a*. Furthermore, 66.67% of AvDGK genes exhibited responsiveness to drought stress, and *AvDGKs* within Cluster II were implicated in the response to low-temperature stress.

We also identified the number and type of cis-elements which were classified into 3 classes (Figure 8B). According to their functions, they were divided into plant growth and development, phytohormone responsive, and abiotic and biotic stress. In the plant growth and development category, there are 41 G-boxes (light responsiveness), of which, *AvDGK5b* accounts for 10 (Figure 8B). In the phytohormone responsive categories, CGTCA-motif (MeJA-responsiveness) and TGACG-motif (MeJA-responsiveness) are two most widely distributed being present in almost all of the 18 genes except *AvDGK19a* (Figure 8B). Additionally, in the abiotic and biotic stress categories, the number of MYC (multi-stress responsiveness) is the most distributed except *AvDGK5a* and *AvDGK18a* (Figure 8B). These results suggested that AvDGK might plays a significant role in plant growth and development, as well as in the response to various stress.

 doi:10.20944/preprints202402.1396.v1

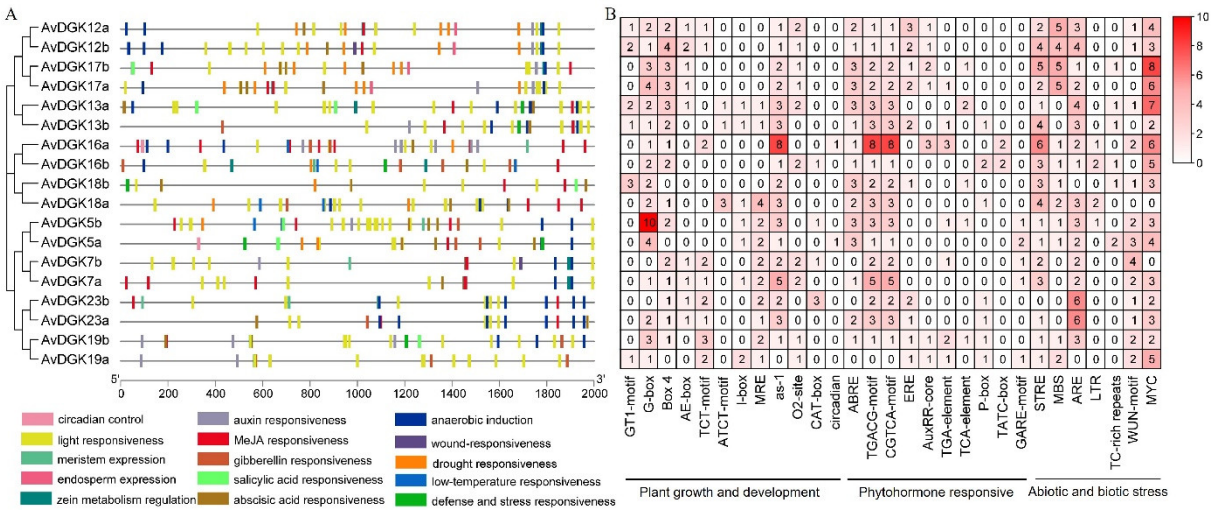

Figure 8. Cis-element analysis of the *AvDGKs*. (**A**) Cis-acting element distribution in promoter regions. Different colored rectangles represent different cis-acting element types. (**B**) Statistics on the number of cis-acting elements associated with plant growth and development, phytohormone and stress responses in the promoter region of *AvDGK* genes.

3.7. Expression Patterns of AvDGKs in kiwifruit

To investigate the expression patterns of *AvDGKs* in kiwifruit, we analyzed the expression levels of the *AvDGK* genes in flesh at different developmental stages of the fruit and in roots under salt stress by utilizing two transcriptome datasets. The expression of *AvDGKs* could be estimated across four fruit stages: stage 1 (mature green fruit stage), stage 2 (breaker fruit stage), stage 3 (colour change fruit stage) and stage 4 (ripe fruit stage) (Figure 9A). The expression profile revealed that *AvDGK16a/b*, *AvDGK17b* and *AvDGK18b* exhibited higher expression levels across different fruit developmental stages. In contrast, genes like *AvDGK7a/b* and *AvDGK13a/b* showed lower expression levels. Additionally, the *AvDGKs* presented different expression profiles during the fruit development (Figure 9A). *AvDGK12a/b* and *AvDGK18a/b* showed decreased expression during the fruit development, while a rise of expression at breaker fruit stage was observed in most other *AvDGK* genes (Figure 9A). Based on the transcriptome data, the expression levels of *AvDGKs* in roots were evaluated after salt treatment 0 h, 12 h, 24 h, and 72 h (Figure 9B). The heatmap results showed that the expression of *AvDGK5a/b*, *AvDGK16a/b*, *AvDGK17a/b*, *AvDGK18a/b* and *AvDGK19a/b* downregulated in response to salt treatment, indicating that the expression of *DGK* in roots was inhibited under salt stress (Figure 9B).

 doi:10.20944/preprints202402.1396.v1

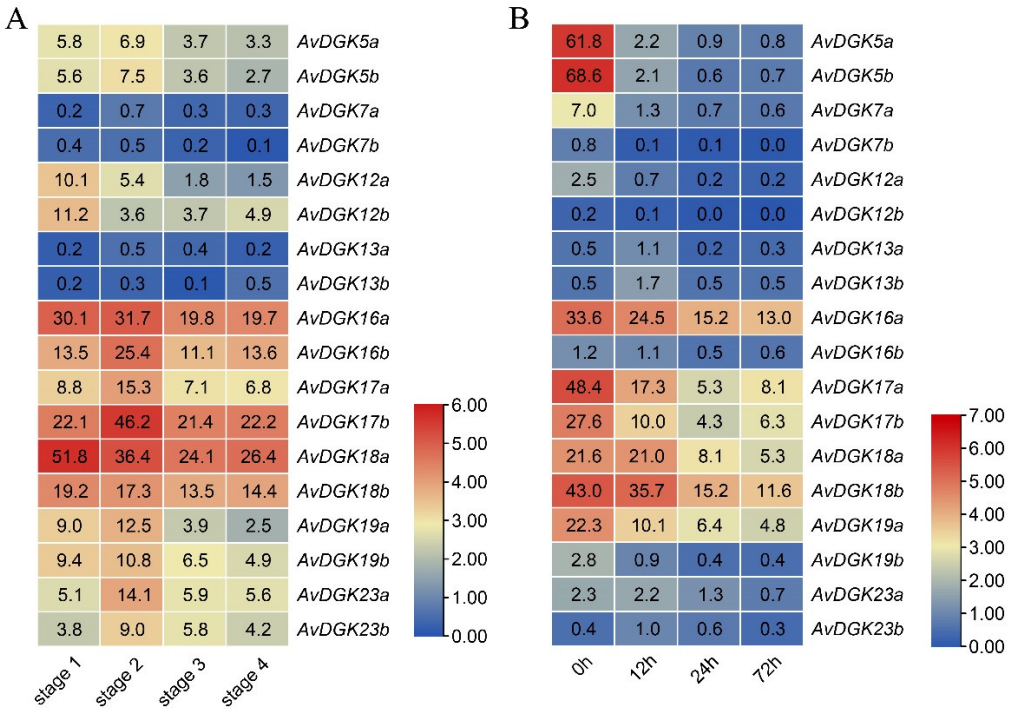

Figure 9. Expression profiles of *AvDGKs* in different fruit stage and under salt stress. (A) Expression profiles of *AvDGKs* in fruit flesh at stage 1 (mature green fruit stage), stage 2 (breaker fruit stage), stage 3 (colour change fruit stage) and stage 4 (ripe fruit stage). (B) Expression profiles of *AvDGKs* in root under salt stress at 0 h, 12 h, 24 h and 72 h.

3.8. RT-qPCR of AvDGKs under waterlogging stress at different time

To further evaluate the role of *AvDGKs* in the response to waterlogging stress, we performed RT-qPCR to obtain insights into expression patterns of *AvDGKs* in roots under waterlogging stress. As shown in Figure 10, the relative expression levels of 15 *AvDGKs* were significantly changed after the treatment. Of these, waterlogging stress significantly induced the expression of *AvDGK12a*, *AvDGK12b*, and *AvDGK18b* (Figure 10). Interestingly, the expression levels of *AvDGK12a* and *AvDGK12b* were slightly different at different treatment time. *AvDGK12b* was rapidly induced by submergence treatment at 6 h, and displayed a trend of decline following the waterlogging stress. Differently, significant upregulation of gene expression for *AvDGK12a* was observed until the submergence treatment 120 h. The expression pattern of *AvDGK18b* post-submergence treatment was similar to that of *AvDGK12b*. Conversely, no significant change in gene expression was detected for *AvDGK18a* following submergence treatment. The result suggested that *AvDGK12b* and *AvDGK18b* played a key role in short-term response while *AvDGK12a* may be involved in regulating the long-term waterlogging stress response. During the stress, *AvDGK5b*, *AvDGK7a*, *AvDGK13b* and *AvDGK16a*, *AvDGK19a/b* and *AvDGK23a/b* showed a similar expression pattern that they sharply decreased to a relatively lower expression level at 6 h or 24 h and upregulated slightly at 120 h (Figure 10). Similarly, the relative expression levels of *AvDGK5a*, *AvDGK7b*, *AvDGK13a* and *AvDGK16b* were significantly reduced and remained at a relatively low level during the submergence stress. Waterlogging stress had no effect on the expression of *AvDGK17a/b*.

 doi:10.20944/preprints202402.1396.v1

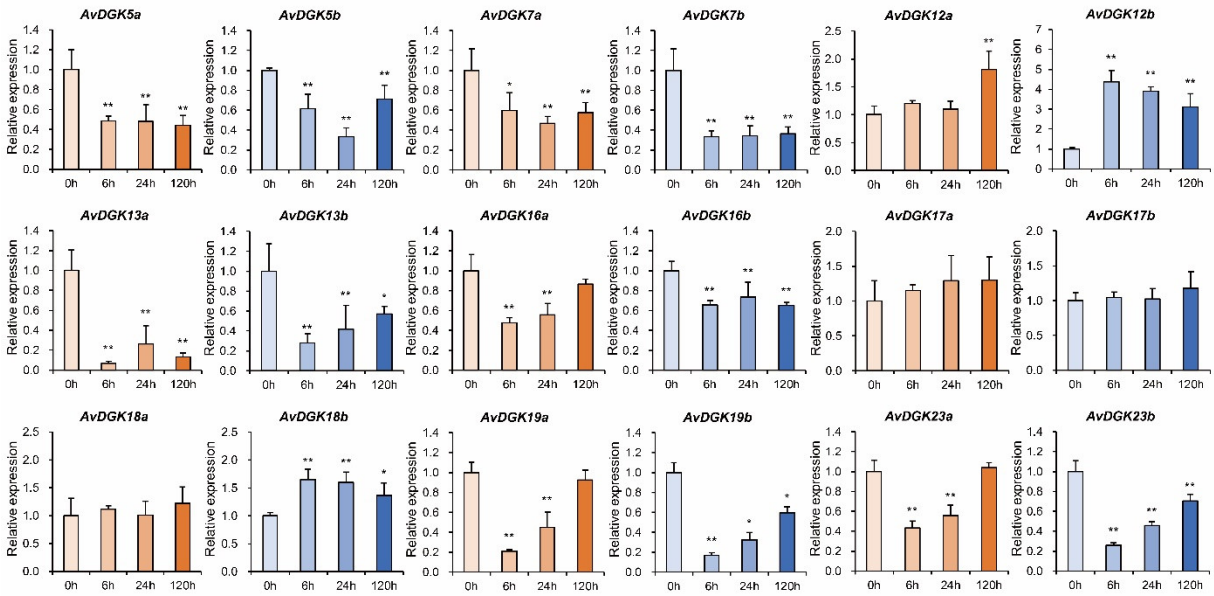

Figure 10. The relative expression levels of *AvDGKs* in the roots under waterlogging stress at different time. Data were shown as means ± SD (n=3) and statistical significance is indicated by *(p<0.05) and **(p<0.01).

4. Discussion

The ability to sense and respond to various environmental stimuli is essential for the growth, development, and survival of plants. Diacylglycerol kinase (DGK) plays a pivotal role in this process by regulating the levels of two crucial signaling molecules, diacylglycerol (DAG) and phosphatidic acid (PA) [12,28]. After lipid phosphorylation of DAG, PA is rapidly produced and accumulates in response to a variety of stresses, such as cold stress, salt stress, hypoxia stress, and submergence [29,55,56]. Upon submergence, it was reported that DGKs and PA derived from DGKs were critical for regulating plant acclimation to submergence [29]. As a submergence-tolerant germplasm, an increasing number of recent studies in *Actinidia valvata* focused on understanding the mechanism of regulating plant tolerance to submergence [33–35,57–59]. However, no reports have addressed the characteristics and potential role of *DGK* gene family members in the waterlogging-tolerance of *Actinidia valvata*. In this study, we identified 18 *AvDGK* members within the *Actinidia valvata* genome which were located on 18 different chromosomes. The number of *AvDGK* genes identified in *Actinidia valvata* genome was relatively higher than the number found in *Arabidopsis thaliana* (7 *AtDGKs*) [14], in *Zea mays* (7 *ZmDGKs*) [21], in *Malus domestica* (8 *MdDGKs*) [19] and in *Populus trichocarpa* (7 *PtDGKs*) [22], but less than those in *Triticum aestivum* (24 *TaDGKs*) [18] and in *Brassica napus* (21 *BnaDGKs*) [17], which may be due to the differences in the size of the genome. The *AvDGKs* encoded proteins ranging from 456~734 amino acids, and these proteins were subcellularly located in the nucleus, chloroplast and cytoplasm.

The grouping and evolutionary relationships of the *DGK* gene family were determined by multiple sequence alignment and the phylogenetic tree construction among monocots and dicots. The AvDGKs were classified into three clusters ,I, II and III, and this classification was confirmed by domain prediction and analysis. The classification of AvDGKs is consistent with previously published reports in other plants and supports the domain conservation and sequence similarity of DGK in plants. In plants, DGKs in Cluster I show a relatively complex domain distribution. They possess the conserved catalytic kinase domain and two C1-type domains which are cysteine-rich domains thought to be responsible for binding the substrate DAG [14]. In addition, an upstream basic region and an extended cysteine-rich (extCRD)-like domain was also found next to the C1 domain. In contrast, Cluster II and III DGKs lack the two C1 domains but still retain the conserved kinase domain. Domain analysis showed that all three clusters display structural characteristics consistent

 doi:10.20944/preprints202402.1396.v1

with previous findings, indicating high conservation of functional domains across different species persists in the evolution of *DGKs*.

Besides the conserved domains, similar exon-intron numbers, motif composition, and subcellular location were found within the clusters. Gene structure of *AvDGK* members in Cluster I and II revealed that they contained seven and twelve exons respectively, the same numbers of exon were also found in wheat [18], common bean [16], soybean [20] and poplar [22]. Conserved exon-intron structure in Cluster I and II indicates that *DGKs* possibly come from a common ancestor and *DGK* genes were strongly affected by the repetitive phenomenon of gene duplication during the evolution [60]. Additionally, different intron and exon patterns were found in *AvDGK* belonging to Cluster III suggesting that the ancestral *AvDGK* gene is likely to have undergone several rounds of intron loss and gain during evolution [61]. These structural differences in Cluster III might confer distinct functional properties.

Diverse gene function is affected significantly by the cis-element located in the promoter regions. Previous studies have reported that cis-elements on the promoters of *DGKs* are associated with multiple stresses such as drought, cold stress and wound stress and hormone responses such as ABA, SA and MeJA [16–18,21,22]. Some of the predictions were confirmed by the expression analysis. *AtDGK1*, *AtDGK2*, *AtDGK3*, and *AtDGK5* genes were upregulated upon exposure to low temperature (4℃) and contributed to cold stress response in *Arabidopsis* [23,55]. Similarly, the expression of *TaDGK1A/B/D* and *TaDGK2D* genes increased significantly at 4℃ in wheat. Under salt stress, *MdDGK4* in apple and *PtDGK3/5* in poplar were induced in the plant salt response [19,22]. In the present study, cis-elements in the promoter of *AvDGK* genes were involved in phytohormone, stress-response, and plant growth and development. The results showed that MeJA responsiveness elements (TGACG-motif and CGTCA motif) were present in almost all *AvDGK* genes, suggesting that *AvDGK* might be associated with MeJA signal transduction and involved in plant defensive responses against environmental stress [62]. Moreover, stress-related response cis-acting elements such as wound stress responsiveness, drought responsiveness, low-temperature responsiveness, anaerobic induction, defense and stress responsiveness were also found in the promoters of *AvDGK* genes. Among them, anaerobic induction element (ARE) was commonly distributed indicating *AvDGK* might play an important role in *A. valvata* upon low oxygen (hypoxia) stress, which is usually caused by root waterlogging and submergence [63].

Gene function is further investigated by determining the expression patterns of *AvDGK* according to the available transcriptome data. Based on the transcriptome data, the expression levels of most *AvDGK* genes increased during breaker fruit stage, suggesting that signal lipids such as DAG and PA are implicated with the ethylene signaling which is activated during fruit ripening [64,65]. It was reported that PA increased during the tomato fruit pericarp ripening [66]. To further explore the role of *AvDGK* under abiotic stress, transcriptome data of *A. valvata* related to salt stress were examined and showed that the expression levels of most *AvDGK* genes in roots decreased with the exception of *AvDGK13a/b*. PA synthesis in response to long-term salt stress was mainly occurred through hydrolysis of PLD, whereas a short-term salt stress might cause PA accumulation via the alternative PLC/DAG kinase pathway [67]. Downregulation of *AvDGK* genes under salt stress might be a strategy for lipid remodeling which could maintain the cell integrity and stability [68], as well as for energy conservation due to the use of ATP as an energy source by DGK to catalyze the conversion of DAG to PA.

Increasing evidence suggests DGK and its product PA are involved in plant acclimation to waterlogging [28,29]. In Arabidopsis, relative transcript levels of *AtDGK1* and *AtDGK5* were upregulated at 10 minutes after submergence [29]. In our study, qRT-PCR analysis was used to examine the relative expression levels of *AvDGK* genes after waterlogging treatment, which showed that the expression of *AvDGK12a*, *AvDGK12b* and *AvDGK18b* were significantly induced under waterlogging stress. Previous studies report that the levels of PA increased significantly in various plant species in response to submergence treatment [69,70], facilitating plant adaptation to hypoxia and improving plant tolerance to submergence [71]. Given that DGK synthesizes PA through the phosphorylation of DAG, expression upregulation of *DGK* was observed in *Arabidopsis* [29] and

 doi:10.20944/preprints202402.1396.v1

Actinidia valvata. Moreover, *AvDGK12b* and *AvDGK18b* were induced rapidly indicating their roles in the immediate response to short-term waterlogging stress, while *AvDGK12a* may be involved in regulating the long-term waterlogging stress response. We propose that *AvDGKs* gene family in the tetraploids *Actinidia valvata* genome promoted PA synthesis and subsequent signal transduction both under short-term and long-term waterlogging stress, which played a key role in enhancing the tolerance of kiwifruit to waterlogging stress.

5. Conclusions

A total of 18 *DGK* genes were identified in the *Actinidia valvata* genome. Based on multiple sequence alignment and phylogenetic analysis, they were divided into three clusters. The motif and functional domains analysis further confirmed the classification and their phylogenetic relationships. The expression levels of *AvDGK* genes including *AvDGK12a*, *AvDGK12b* and *AvDGK18b* were significantly upregulated under waterlogging stress. Thus, our findings provide a theoretical foundation for further exploration of candidate genes for enhancing kiwifruit tolerance to waterlogging stress.

Supplementary Materials: The following supporting information can be downloaded at the website of this paper posted on Preprints.org. Figure S1: Amino acid similarity analysis of the AvDGK proteins with DGK from *Arabidopsis thaliana*; Figure S2: The secondary structure of the AvDGKs; Figure S3: 3D models of AvDGK proteins. 3D models were constructed using the online Phyre2 server with default mode; Figure S4: Sequence logos for 10 conserved motifs identified in the AvDGKs; Figure S5: Numbers of exon/intron in *AvDGK* gene family; Table S1: The primer pairs used in RT-qPCR analysis; Table S2: Chromosomal location of the *AvDGK* genes; Table S3: The secondary structure analysis of the AvDGK proteins; Table S4: Duplication events identified in *AvDGKs*.

Author Contributions: Conceptualization, M.Z. and C.L.; methodology, M.Z.; software, F.W. and B.Q.; validation, M.Z., C.L. and F.W.; formal analysis, J.L.; investigation, M.Z., J.G. and K.Y.; resources, S.L.; data curation, Q.M.; writing-original draft preparation, M.Z.; writing-review and editing, C.L.; visualization, C.L.; supervision, H.G.; project administration, C.L.; funding acquisition, C.L. All authors have read and agreed to the published version of the manuscript.

Funding: This work was supported by the National Natural Science Foundation of China (32060643, 32060666), Guangxi Science and Technology Program (GuikeAD23026228), the Guilin Innovation Platform and Talent Plan (20220125-7), the Fundamental Research Fund of Guangxi Institute of Botany (23008), Guangxi Science and Technology Major Project (Guike AA23023008), the Earmarked Fund for China Agriculture Research System (nycytxgxcxtd-2023-13-01) and the Doctoral Research Funding from Shangluo University (17SKY016).

Data Availability Statement: Not applicable.

Conflicts of Interest: The authors declare no conflicts of interest.

References

1. Yao, S.; Kim, S.; Li, J.; Tang, S.; Wang, X. Phosphatidic acid signaling and function in nuclei. *Prog. Lipid Res.* **2024**, *93*, 101267, doi:https://doi.org/10.1016/j.plipres.2023.101267.
2. Kong, L.; Ma, X.; Zhang, C.; Kim, S.; Li, B.; Xie, Y.; Yeo, I.; Thapa, H.; Chen, S.; Devarenne, T.P.; et al. Dual phosphorylation of DGK5-mediated PA burst regulates ROS in plant immunity. *Cell* **2024**, *187*, 609-623.e621, doi:https://doi.org/10.1016/j.cell.2023.12.030.
3. Ali, U.; Lu, S.; Fadlalla, T.; Iqbal, S.; Yue, H.; Yang, B.; Hong, Y.; Wang, X.; Guo, L. The functions of phospholipases and their hydrolysis products in plant growth, development and stress responses. *Prog. Lipid Res.* **2022**, *86*, 101158, doi:https://doi.org/10.1016/j.plipres.2022.101158.
4. Hong, Y.; Zhao, J.; Guo, L.; Kim, S.; Deng, X.; Wang, G.; Zhang, G.; Li, M.; Wang, X. Plant phospholipases D and C and their diverse functions in stress responses. *Prog. Lipid Res.* **2016**, *62*, 55–74, doi:https://doi.org/10.1016/j.plipres.2016.01.002.
5. Kim, S.; Wang, X. Phosphatidic acid: an emerging versatile class of cellular mediators. *Essays. Biochem.* **2020**, *64*, 533–546, doi:https://doi.org/10.1042/EBC20190089.
6. Testerink, C.; Munnik, T. Phosphatidic acid: a multifunctional stress signaling lipid in plants. *Trends Plant Sci.* **2005**, *10*, 368–375, doi:https://doi.org/10.1016/j.tplants.2005.06.002.
7. Fan, B.; Liao, K.; Wang, L.; Shi, L.; Zhang, Y.; Xu, L.; Zhou, Y.; Li, J.; Chen, Y.; Chen, Q.; et al. Calcium-dependent activation of CPK12 facilitates its cytoplasm-to-nucleus translocation to potentiate plant hypoxia sensing by phosphorylating ERF-VII transcription factors. *Mol. Plant* **2023**, *16*, 979–998, doi:https://doi.org/10.1016/j.molp.2023.04.002.

8. Lindberg, S.; Premkumar, A.; Rasmussen, U.; Schulz, A.; Lager, I. Phospholipases AtPLDζ1 and AtPLDζ2 function differently in hypoxia. *Physiol. Plant* **2018**, *162*, 98–108, doi:https://doi.org/10.1111/ppl.12620.
9. Kolesnikov, Y.; Kretynin, S.; Bukhonska, Y.; Pokotylo, I.; Ruelland, E.; Martinec, J.; Kravets, V. Phosphatidic acid in plant hormonal signaling: from target proteins to membrane conformations. *Int. J. Mol. Sci.* **2022**, *23*, 3227, doi:https://doi.org/10.3390/ijms23063227.
10. Park, J.; Gu, Y.; Lee, Y.; Yang, Z.; Lee, Y. Phosphatidic acid induces leaf cell death in Arabidopsis by activating the rho-related small G protein GTPase-mediated pathway of reactive oxygen species generation. *Plant Physiol.* **2004**, *134*, 129–136, doi:https://doi.org/10.1104/pp.103.031393.
11. Scholz, P.; Pejchar, P.; Fernkorn, M.; Škrabálková, E.; Pleskot, R.; Blersch, K.; Munnik, T.; Potocký, M.; Ischebeck, T. DIACYLGLYCEROL KINASE 5 regulates polar tip growth of tobacco pollen tubes. *New Phytol.* **2022**, *233*, 2185–2202, doi:https://doi.org/10.1111/nph.17930.
12. Kue Foka, I.C.; Ketehouli, T.; Zhou, Y.; Li, X.; Wang, F.; Li, H. The emerging roles of diacylglycerol kinase (DGK) in plant stress tolerance, growth, and development. *Agronomy* **2020**, *10*, 1375, doi:https://doi.org/10.3390/agronomy10091375.
13. Escobar Sepúlveda, H.F.; Trejo Téllez, L.I.; Pérez Rodríguez, P.; Hidalgo Contreras, J.V.; Gómez Merino, F.C. Diacylglycerol kinases are widespread in higher plants and display inducible gene expression in response to beneficial elements, metal, and metalloid ions. *Front. Plant Sci.* **2017**, *8*, doi: https://doi.org/10.3389/fpls.2017.00129.
14. Arisz, S.A.; Testerink, C.; Munnik, T. Plant PA signaling via diacylglycerol kinase. *Biochim. Biophys. Acta.* **2009**, *1791*, 869–875, doi:https://doi.org/10.1016/j.bbalip.2009.04.006.
15. Ge, H.; Chen, C.; Jing, W.; Zhang, Q.; Wang, H.; Wang, R.; Zhang, W. The rice diacylglycerol kinase family: functional analysis using transient RNA interference. *Front. Plant Sci.* **2012**, *3*, doi:https://doi.org/10.3389/fpls.2012.00060.
16. Yeken, M.Z.; Özer, G.; Çiftçi, V. Genome-wide identification and expression analysis of *DGK* (diacylglycerol kinase) genes in common bean. *J. Plant Growth Regul.* **2023**, *42*, 2558–2569, doi:https://doi.org/10.1007/s00344-022-10726-x.
17. Tang, F.; Xiao, Z.; Sun, F.; Shen, S.; Chen, S.; Chen, R.; Zhu, M.; Zhang, Q.; Du, H.; Lu, K.; et al. Genome-wide identification and comparative analysis of diacylglycerol kinase (*DGK*) gene family and their expression profiling in *Brassica napus* under abiotic stress. *BMC Plant Biol.* **2020**, *20*, 473, doi:https://doi.org/10.1186/s12870-020-02691-y.
18. Jia, X.; Si, X.; Jia, Y.; Zhang, H.; Tian, S.; Li, W.; Zhang, K.; Pan, Y. Genomic profiling and expression analysis of the diacylglycerol kinase gene family in heterologous hexaploid wheat. *PeerJ* **2021**, *9*, e12480, doi:https://doi.org/10.7717/peerj.12480.
19. Li, Y.; Tan, Y.; Shao, Y.; Li, M.; Ma, F. Comprehensive genomic analysis and expression profiling of diacylglycerol kinase gene family in *Malus prunifolia* (Willd.) Borkh. *Gene* **2015**, *561*, 225–234, doi:https://doi.org/10.1016/j.gene.2015.02.029.
20. Carther, K.F.I.; Ketehouli, T.; Ye, N.; Yang, Y.H.; Wang, N.; Dong, Y.Y.; Yao, N.; Liu, X.M.; Liu, W.C.; Li, X.W.; et al. Comprehensive genomic analysis and expression profiling of diacylglycerol kinase (*DGK*) gene family in soybean (*Glycine max*) under abiotic stresses. *Int. J. Mol. Sci.* **2019**, *20*, 1361, doi:https://doi.org/10.3390/ijms20061361.
21. Gu, Y.; Zhao, C.; He, L.; Yan, B.; Dong, J.; Li, Z.; Yang, K.; Xu, J. Genome-wide identification and abiotic stress responses of *DGK* gene family in maize. *J. Plant Biochem. Biotechnol.* **2018**, *27*, 156–166, doi:https://doi.org/10.1007/s13562-017-0424-8.
22. Wang, H.; Yan, Z.; Yang, M.; Gu, L. Genome-wide identification and characterization of the diacylglycerol kinase (DGK) gene family in *Populus trichocarpa*. *Physiol. Mol. Plant Pathol.* **2023**, *127*, 102121, doi:https://doi.org/10.1016/j.pmpp.2023.102121.
23. Gómez Merino, F.C.; Brearley, C.A.; Ornatowska, M.; Abdel Haliem, M.E.F.; Zanor, M.I.; Mueller Roeber, B. AtDGK2, a novel diacylglycerol kinase from *Arabidopsis thaliana*, phosphorylates 1-stearoyl-2-arachidonoyl-sn-glycerol and 1,2-dioleoyl-sn-glycerol and exhibits cold-inducible gene expression. *J. Biol. Chem.* **2004**, *279*, 8230–8241, doi:https://doi.org/10.1074/jbc.M312187200.
24. Vaultier, M.N.; Cantrel, C.; Guerbette, F.; Boutté, Y.; Vergnolle, C.; Çiçek, D.; Bolte, S.; Zachowski, A.; Ruelland, E. The hydrophobic segment of *Arabidopsis thaliana* cluster I diacylglycerol kinases is sufficient to target the proteins to cell membranes. *FEBS Letters* **2008**, *582*, 1743–1748, doi:https://doi.org/10.1016/j.febslet.2008.04.042.
25. Snedden, W.A.; Blumwald, E. Alternative splicing of a novel diacylglycerol kinase in tomato leads to a calmodulin-binding isoform. *Plant J.* **2000**, *24*, 317–326, doi:https://doi.org/10.1046/j.1365-313x.2000.00877.x.
26. Gómez Merino, F.C.; Arana Ceballos, F.A.; Trejo Téllez, L.I.; Skirycz, A.; Brearley, C.A.; Dörmann, P.; Mueller Roeber, B. Arabidopsis AtDGK7, the smallest member of plant diacylglycerol kinases (DGKs), displays unique biochemical features and saturates at low substrate concentration. *J. Biol. Chem.* **2005**, *280*, 34888 - 34899, doi:https://doi.org/10.1074/jbc.M506859200.

27. Yuan, S.; Kim, S.; Deng, X.; Hong, Y.; Wang, X. Diacylglycerol kinase and associated lipid mediators modulate rice root architecture. *New Phytol.* **2019**, *223*, 261–276, doi:https://doi.org/10.1111/nph.15801.
28. Li, J.; Yao, S.; Kim, S.; Wang, X. Lipid phosphorylation by a diacylglycerol kinase suppresses ABA biosynthesis to regulate plant stress responses. *Mol. Plant* **2024**, *17*, 342–358, doi:https://doi.org/10.1016/j.molp.2024.01.003.
29. Zhou, Y.; Zhou, D.; Yu, W.; Shi, L.; Zhang, Y.; Lai, Y.; Huang, L.; Qi, H.; Chen, Q.; Yao, N.; et al. Phosphatidic acid modulates MPK3- and MPK6-mediated hypoxia signaling in Arabidopsis. *Plant Cell.* **2021**, *34*, 889–909, doi:https://doi.org/10.1093/plcell/koab289.
30. Huang, H. Chapter 1 - Systematics and genetic variation of *Actinidia*. In *Kiwifruit*, Huang, H., Ed.; Academic Press: San Diego, 2016; pp. 9–44.
31. Ferguson, A.R.; Huang, H. Genetic resources of Kiwifruit: domestication and breeding. In *Horticultural Reviews*; 2007; pp. 1–121.
32. Li, X.; Li, J.; Soejarto, D.D. Advances in the study of the systematics of *Actinidia* Lindley. *Front. Biol. China* **2009**, *4*, 55–61, doi:https://doi.org/10.1007/s11515-008-0110-2.
33. Gao, M.; Gai, C.; Li, X.; Feng, X.; Lai, R.; Song, Y.; Zeng, R.; Chen, D.; Chen, Y. Waterlogging tolerance of *Actinidia valvata* Dunn is associated with high activities of pyruvate decarboxylase, alcohol dehydrogenase and antioxidant enzymes. *Plants* **2023**, *12*, 2872, doi:https://doi.org/10.3390/plants12152872.
34. Bai, D.; Li, Z.; Hu, C.; Zhang, Y.; Muhammad, A.; Zhong, Y.; Fang, J. Transcriptome-wide identification and expression analysis of *ERF* family genes in *Actinidia valvata* during waterlogging stress. *Scientia Hortic.* **2021**, *281*, 109994, doi:https://doi.org/10.1016/j.scienta.2021.109994.
35. Li, Z.; Bai, D.; Zhong, Y.; Abid, M.; Qi, X.; Hu, C.; Fang, J. Physiological responses of two contrasting Kiwifruit (*Actinidia* spp.) rootstocks against waterlogging stress. *Plants* **2021**, *10*, 2586, doi:https://doi.org/10.3390/plants10122586.
36. Lamesch, P.; Berardini, T.Z.; Li, D.; Swarbreck, D.; Wilks, C.; Sasidharan, R.; Muller, R.; Dreher, K.; Alexander, D.L.; Garcia-Hernandez, M.; et al. The Arabidopsis Information Resource (TAIR): improved gene annotation and new tools. *Nucleic Acids Res.* **2011**, *40*, D1202-D1210, doi:https://doi.org/10.1093/nar/gkr1090.
37. Mistry, J.; Chuguransky, S.; Williams, L.; Qureshi, M.; Salazar, Gustavo A.; Sonnhammer, E.L.L.; Tosatto, S.C.E.; Paladin, L.; Raj, S.; Richardson, L.J.; et al. Pfam: The protein families database in 2021. *Nucleic Acids Res.* **2020**, *49*, D412-D419, doi:https://doi.org/10.1093/nar/gkaa913.
38. Potter, S.C.; Luciani, A.; Eddy, S.R.; Park, Y.; Lopez, R.; Finn, R.D. HMMER web server: 2018 update. *Nucleic Acids Res.* **2018**, *46*, W200-W204, doi:https://doi.org/10.1093/nar/gky448.
39. Chou, K.; Shen, H. Plant-mPLoc: A top-down strategy to augment the power for predicting plant protein subcellular localization. *PLoS One* **2010**, *5*, e11335, doi:https://doi.org/10.1371/journal.pone.0011335.
40. Geourjon, C.; Deléage, G. SOPMA: significant improvements in protein secondary structure prediction by consensus prediction from multiple alignments. *Bioinformatics* **1995**, *11*, 681–684, doi:https://doi.org/10.1093/bioinformatics/11.6.681.
41. Kelley, L.A.; Mezulis, S.; Yates, C.M.; Wass, M.N.; Sternberg, M.J.E. The Phyre2 web portal for protein modeling, prediction and analysis. *Nat. Protoc.* **2015**, *10*, 845–858, doi:https://doi.org/10.1038/nprot.2015.053.
42. Liu, W.; Xie, Y.; Ma, J.; Luo, X.; Nie, P.; Zuo, Z.; Lahrmann, U.; Zhao, Q.; Zheng, Y.; Zhao, Y.; et al. IBS: an illustrator for the presentation and visualization of biological sequences. *Bioinformatics* **2015**, *31*, 3359–3361, doi:https://doi.org/10.1093/bioinformatics/btv362.
43. Goodstein, D.M.; Shu, S.; Howson, R.; Neupane, R.; Hayes, R.D.; Fazo, J.; Mitros, T.; Dirks, W.; Hellsten, U.; Putnam, N.; et al. Phytozome: a comparative platform for green plant genomics. *Nucleic Acids Res.* **2011**, *40*, D1178-D1186, doi:https://doi.org/10.1093/nar/gkr944.
44. Letunic, I.; Bork, P. Interactive Tree Of Life (iTOL) v5: an online tool for phylogenetic tree display and annotation. *Nucleic Acids Res.* **2021**, *49*, W293-W296, doi:https://doi.org/10.1093/nar/gkab301.
45. Robert, X.; Gouet, P. Deciphering key features in protein structures with the new ENDscript server. *Nucleic Acids Res.* **2014**, *42*, W320-W324, doi:https://doi.org/10.1093/nar/gku316.
46. Bailey, T.L.; Johnson, J.; Grant, C.E.; Noble, W.S. The MEME Suite. *Nucleic Acids Res.* **2015**, *43*, W39-W49, doi:https://doi.org/10.1093/nar/gkv416.
47. Chen, C.; Wu, Y.; Li, J.; Wang, X.; Zeng, Z.; Xu, J.; Liu, Y.; Feng, J.; Chen, H.; He, Y.; et al. TBtools-II: A "one for all, all for one" bioinformatics platform for biological big-data mining. *Mol. Plant* **2023**, *16*, 1733–1742, doi:https://doi.org/10.1016/j.molp.2023.09.010.
48. Chao, J.; Li, Z.; Sun, Y.; Aluko, O.O.; Wu, X.; Wang, Q.; Liu, G. MG2C: a user-friendly online tool for drawing genetic maps. *Mol. Hortic.* **2021**, *1*, 16, doi:https://doi.org/10.1186/s43897-021-00020-x.
49. Wang, Y.; Tang, H.; DeBarry, J.D.; Tan, X.; Li, J.; Wang, X.; Lee, T.-h.; Jin, H.; Marler, B.; Guo, H.; et al. MCScanX: a toolkit for detection and evolutionary analysis of gene synteny and collinearity. *Nucleic Acids Res.* **2012**, *40*, e49-e49, doi:https://doi.org/10.1093/nar/gkr1293.

50. Lescot, M.; Déhais, P.; Thijs, G.; Marchal, K.; Moreau, Y.; Van de Peer, Y.; Rouzé, P.; Rombauts, S. PlantCARE, a database of plant cis-acting regulatory elements and a portal to tools for in silico analysis of promoter sequences. *Nucleic Acids Res.* **2002**, *30*, 325–327, doi:https://doi.org/10.1093/nar/30.1.325.
51. Hou, Y.; Fan, C.; Sun, J.; Chang, Y.; Lu, J.; Sun, J.; Wang, C.; Liu, J. Genome-wide Identification, evolution, and expression analysis of the *TCP* gene family in rose (*Rosa chinensis* Jacq.). *Horticulturae* **2022**, *8*, 961, doi:https://doi.org/10.3390/horticulturae8100961.
52. Livak, K.J.; Schmittgen, T.D. Analysis of relative gene expression data using real-time quantitative PCR and the 2(-Delta Delta C(T)) method. *Methods (San Diego, Calif.)* **2001**, *25*, 402–408, doi:https://doi.org/10.1006/meth.2001.1262.
53. Zhang, Z. KaKs_calculator 3.0: calculating selective pressure on coding and non-coding sequences. *Genomics Proteomics Bioinformatics.* **2022**, *20*, 536–540, doi:https://doi.org/10.1016/j.gpb.2021.12.002.
54. Zhang, Z.; Li, J.; Zhao, X.Q.; Wang, J.; Wong, G.K.; Yu, J. KaKs_Calculator: calculating Ka and Ks through model selection and model averaging. *Genomics Proteomics Bioinformatics.* **2006**, *4*, 259–263, doi:https://doi.org/10.1016/S1672-0229(07)60007-2.
55. Arisz, S.A.; van Wijk, R.v.; Roels, W.; Zhu, J.; Haring, M.A.; Munnik, T. Rapid phosphatidic acid accumulation in response to low temperature stress in Arabidopsis is generated through diacylglycerol kinase. *Front. Plant Sci.* **2013**, *4*, doi:https://doi.org/10.3389/fpls.2013.00001.
56. Shen, L.; Zhuang, B.; Wu, Q.; Zhang, H.; Nie, J.; Jing, W.; Yang, L.; Zhang, W. Phosphatidic acid promotes the activation and plasma membrane localization of MKK7 and MKK9 in response to salt stress. *Plant Sci.* **2019**, *287*, 110190, doi:https://doi.org/10.1016/j.plantsci.2019.110190.
57. Gao, Y.; jiang, Z.; Shi, M.; Zhou, Y.; Huo, L.; Li, X.; Xu, K. Comparative transcriptome provides insight into responding mechanism of waterlogging stress in *Actinidia valvata* Dunn. *Gene* **2022**, *845*, 146843, doi:https://doi.org/10.1016/j.gene.2022.146843.
58. Li, Z.; Zhong, Y.; Bai, D.; Lin, M.; Qi, X.; Fang, J. Comparative analysis of physiological traits of three *Actinidia valvata* Dunn genotypes during waterlogging and post-waterlogging recovery. *Hortic. Environ. Biote.* **2020**, *61*, 825–836, doi:https://doi.org/10.1007/s13580-020-00276-0.
59. Li, Z.; Bai, D.; Zhong, Y.; Lin, M.; Sun, L.; Qi, X.; Hu, C.; Fang, J. Full-Length transcriptome and RNA-Seq analyses reveal the mechanisms underlying waterlogging tolerance in Kiwifruit (*Actinidia valvata*). *Int. J. Mol. Sci.* **2022**, *23*, 3237, doi:https://doi.org/10.3390/ijms23063237.
60. Lynch, M.; O'Hely, M.; Walsh, B.; Force, A. The probability of preservation of a newly arisen gene duplicate. *Genetics* **2001**, *159*, 1789–1804, doi:https://doi.org/10.1093/genetics/159.4.1789.
61. Rogozin, I.B.; Wolf, Y.I.; Sorokin, A.V.; Mirkin, B.G.; Koonin, E.V. Remarkable interkingdom conservation of intron positions and massive, lineage-specific intron loss and gain in eukaryotic evolution. *Curr. Biol.* **2003**, *13*, 1512–1517, doi:https://doi.org/10.1016/S0960-9822(03)00558-X.
62. Santino, A.; Taurino, M.; De Domenico, S.; Bonsegna, S.; Poltronieri, P.; Pastor, V.; Flors, V. Jasmonate signaling in plant development and defense response to multiple (a)biotic stresses. *Plant Cell Rep.* **2013**, *32*, 1085–1098, doi:https://doi.org/10.1007/s00299-013-1441-2.
63. León, J.; Castillo, M.C.; Gayubas, B. The hypoxia–reoxygenation stress in plants. *J. Exp. Bot.* **2020**, *72*, 5841–5856, doi:https://doi.org/10.1093/jxb/eraa591.
64. Chen, T.; Qin, G.; Tian, S. Regulatory network of fruit ripening: current understanding and future challenges. *New Phytol.* **2020**, *228*, 1219–1226, doi:https://doi.org/10.1111/nph.16822.
65. Bhardwaj, S.; Verma, T.; Kapoor, D. Ethylene and regulation of metabolites in plants. In *Ethylene in Plant Biology*; 2022; pp. 32–48.
66. Whitaker, B.D.; Smith, D.L.; Green, K.C. Characterization of a phospholipase Dα cDNA from tomato fruit. *Biochem. Soc. Trans.* **2000**, *28*, 819–821, doi:https://doi.org/10.1042/bst0280819.
67. Guo, Q.; Liu, L.; Barkla, B.J. Membrane lipid remodeling in response to salinity. *Int. J. Mol. Sci.* **2019**, *20*, 4264, doi: https://doi.org/10.3390/ijms20174264.
68. Ge, S.; Liu, D.; Chu, M.; Liu, X.; Wei, Y.; Che, X.; Zhu, L.; He, L.; Xu, J. Dynamic and adaptive membrane lipid remodeling in leaves of sorghum under salt stress. *Crop J.* **2022**, *10*, 1557–1569, doi:https://doi.org/10.1016/j.cj.2022.03.006.
69. Xu, L.; Pan, R.; Zhou, M.; Xu, Y.; Zhang, W. Lipid remodelling plays an important role in wheat (*Triticum aestivum*) hypoxia stress. *Funct. Plant Biol.* **2020**, *47*, 58–66, doi:https://doi.org/10.1071/FP19150.
70. Wang, M.; Shen, Y.; Tao, F.; Yang, S.; Li, W. Submergence induced changes of molecular species in membrane lipids in *Arabidopsis thaliana*. *Plant Divers.* **2016**, *38*, 156–162, doi:https://doi.org/10.1016/j.pld.2016.05.006.
71. Xie, L.; Zhou, Y.; Chen, Q.; Xiao, S. New insights into the role of lipids in plant hypoxia responses. *Prog. Lipid Res.* **2021**, *81*, 101072, doi:https://doi.org/10.1016/j.plipres.2020.101072.

 doi:10.20944/preprints202402.1396.v1

disclaim responsibility for any injury to people or property resulting from any ideas, methods, instructions or products referred to in the content.